# A CONDITION-BASED PROBABILISTIC SAFETY ASSESSMENT FRAMEWORK FOR THE ESTIMATION OF THE FREQUENCY OF CORE DAMAGE DUE TO AN INDUCED STEAM GENERATOR TUBE RUPTURE

Federico Antonello[1], Francesco Di Maio[1], Enrico Zio[1,2,3]

[1]*Energy Department, Politecnico di Milano, Via Lambruschini 4, 20156, Milan, Italy.*
[2]*MINES ParisTech, PSL Research University, CRC, Sophia Antipolis, France.*
[3]*Eminent Scholar, Department of Nuclear Engineering, College of Engineering, Kyung Hee University, Republic of Korea*

*Condition-Based Probabilistic Safety Assessment (CB-PSA) makes use of information on the components health conditions during operation to dynamically update the risk estimators (e.g., Core Damage Frequency (CDF)). In this paper, we perform a CB-PSA for controlling the risk of a Steam Line Break (SLB)-induced Steam Generator Tube Rupture (SGTR) accident scenario in a Pressurized Water Reactor (PWR) and use the outcome for optimizing the maintenance.*

## I. INTRODUCTION

Probabilistic Safety Assessment (PSA) is a systematic framework to quantify risk indicators, such as the Core Damage Frequency (CDF) for Nuclear Power Plants (NPPs) (Refs. 1, 2, 3, 4, 5).

A Condition-Based PSA (CB-PSA) framework has been previously proposed by the authors in (Ref. 6) to update the plant risk profile, taking in to account the monitored conditions of the components and systems. This requires integrating the conventional PSA techniques like Event Tree Analysis (ETA) and Fault Tree Analyses (FTA) with condition monitoring techniques (Refs 2, 7, 8, 9, 10, 11). Figure 1 compares the failure probability provided by a conventional PSA to the condition-dependent failure probability provided by a CB-PSA, which makes use of condition-monitoring data (e.g., the state indicator values).

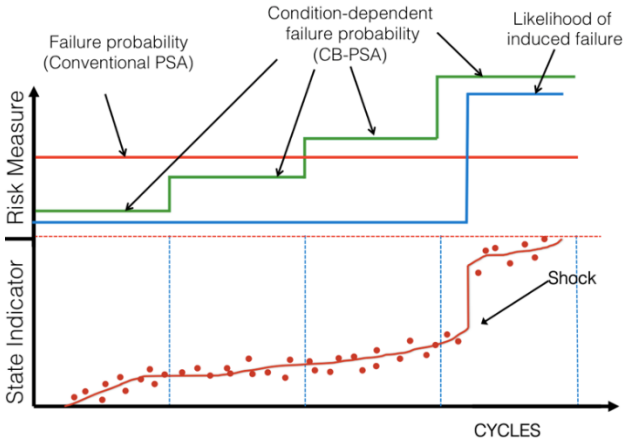


Figure 1. Comparison between failure probability provided by conventional PSA and condition-dependent failure probability provided by CB-PSA.

The remainder of this paper is as follows: in Section 2, the case study of a SLB-induced SGTR in a pressurized water reactor (PWR) is considered and the models used to implement the CB-PSA are described; in Section 3, the CB-PSA framework is presented, while Section 4 draws some conclusions.

## II. INDUCED SGTR

SGTR can be either an induced or a spontaneous phenomenon: the former consists in the break of one or more SG tubes that is triggered by other internal events, such as a SLB, whereas the latter is not triggered by anything but emerges from degradation of the tubes (Ref. 12).

Figure 2 shows the ET that follows to a SLB Initiating Event (IE) that can originate an induced SGTR (see Table I for ET headers description).

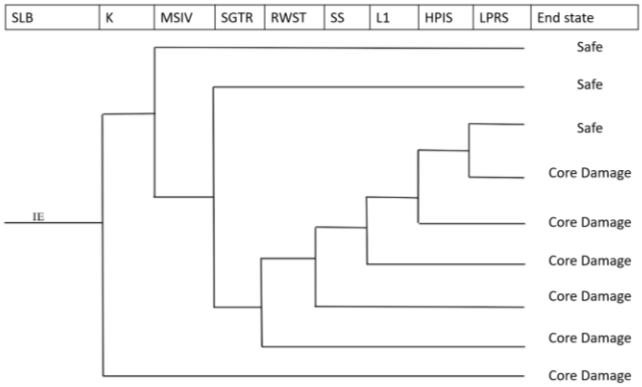


Figure 2.ET of a SLB-induced SGTR (Ref. 14).

A SLB initiates the sequence whose first line response is a reactor trip (K); the successful plant shutdown and the closure of a Main Steam Isolation Valve (MSIV) results in a successful prevention of core meltdown; in case of MSIV failure, if the integrity of the SG tubes is guaranteed, meltdown is also avoided. However, if the SG tubes rupture (SGTR) occurs, a series of safety systems are called

in operation to counteract the core meltdown: failures of water supply from either the Refueling Water Storage Tank (RWST), the Safety injection System actuator signal (SS), the auxiliary feed-water actuation and secondary cooling (L1) or the High Pressure Injection System (HPIS) leads to an early core meltdown; the last barrier towards core damage is the Low Pressure Recirculation (LPRS). Traditionally, the probabilities of occurrence of the events along the sequences in the ET (as well as for the SGTR) are estimated from statistical analysis of reliability data, expert judgement (Ref. 10) and extensive operational experience (Ref. 15).

Table I lists the probability of the failure events along the ET of Figure 2, together with their uncertainties (Ref. 14, 16).

Table I. Failure probabilities for the accidents considered

| **Event Acronym** | **Event Description** | **Frequency and Probability of Failure-On-Demand** | **Minimum Value** | **Maximum Value** |
|---|---|---|---|---|
| SLB (IE) | Steam Line Break | 1.88E-3/year | 1.88E-4/years | 1.88E-2/years |
| K | Reactor trip | 1.8E-4 | 1.8E-5 | 1.8E-3 |
| MSIV | Main Steam Isolation Valve failure | 1.9E-2 | 1.9E-3 | 1.9E-1 |
| SGTR | Steam Generator Tube Rupture given overpressure gradient | 9E-3 | 0 | 1 |
| RWST | Refueling Water Storage Tank failure | 2.4E-8 | 2.4E-9 | 2.4E-7 |
| SS | Failure of the Safety Injection System actuation signal | 2.2E-5 | 2.2E-6 | 2.2E-4 |
| L1 | Failure of the auxiliary feed-water actuation and secondary cooling | 3.4e-5 | 2.2E-6 | 2.2E-4 |
| HPIS | High Pressure Injection System failure | 2.1E-8 | 2.1E-9 | 2.1E-7 |
| LPRS | Low Pressure Recirculation System failure | 4.6E-4 | 4.6E-5 | 4.6E-3 |

Under this assumption, the CDF for a conventional PSA turns out to be equal to 1.3E-6 per year and is considered constant throughout the 40 years lifetime of the NPP (Ref. 15).

## II.A. The Steam Generator

We consider the SG of the Zion NPP, 3.6 m and 21 m in diameter and height, respectively, weighting 800 t and equipped with a bundle of 3592 inverted U tubes with an outside diameter of 22.23 mm and a wall thickness of 1.27 mm (Ref. 14). A detailed list of Zion NPP parameters values is given in Table II: among these, it is worth mentioning the primary loop nominal pressure that is equal to 15.2 MPa, and the secondary loop nominal pressure that is equal to 6.9 MPa. The hot leg nominal temperature is 330°C, while the nominal cold leg temperature is 288°C.

Table II. Parameters of the Zion PWR NPP under consideration

| **NPP Operating Conditions** | |
|---|---|
| Nominal Power $W_{nom}$ | 1110 $MW_e$ |
| Primary side pressure $P_{in,nom}$ | 15.2 MPa |
| Secondary side pressure $P_{out,nom}$ | 6.9 MPa |
| Number of tubes $N_{tb}$ | 3592 |

## II.B. The SLB-induced SGTR model

The SLB is an accident event that leads the secondary side of the SG to complete depressurization, causing an unexpected increase of the pressure difference ΔP between the inner and outer sides of the SG tubes. This shocking event insists on (and affects) the state of the SG tubes, because the larger the tube degradation, the larger the likelihood of tube ruptures due to an overpressure that the tube cannot withstand. The CB-PSA approach presented in this work will give due account to a model that is capable to consider both the aging and degradation of the SG during the whole plant lifetime and the response of the tube to the extreme operational condition caused by the SLB.

The degradation mechanism that affects the SG is here assumed to be due to a Stress Corrosion Cracking (SCC) phenomenon (Ref. 17), that proceeds upon crack onset, by formation and propagation of cracks inside the tube well.

The crack onset probability is modeled with a Weibull distribution υ( λ, b), where λ and *b* are estimated equal to 30.1609 and 0.3654, respectively (see (Refs. 6, 18), for further details), based on the actual data collected in the Zion Plant.

According to (Ref. 17), microcracks reach the critical crack length of 0.1 mm (i.e., the minimum length that will make the crack propagating faster) in about 9.3 years (with standard deviation of 3.2 years) at the operating temperature of 330°C.

The crack propagation is described by the Scott model (Ref. 17), which is an empirical model that provides the crack length growth rate $\frac{da}{dt}$ as a function of the stress intensity factor *k*

$$\frac{da}{dt} = \alpha \cdot (k - k_{th})^{\beta} \quad (1)$$

where

$$k = F\sigma\sqrt{\pi \frac{a}{2}} \quad (2)$$

and $\alpha$, $\beta$, $k_{th}$ and $F$ are constants that depend on the material (listed in Table III, for Alloy 600 MA when wet by water at 330°C (Ref. 17)).

The stress crack tip σ is proportional to the pressure difference ΔP between the inner and the outer sides of the SG tube, the outer diameter $d$ and the thickness of the tube $t$ (given in Table IV) as in Eq. (3).

$$\sigma = \Delta P \cdot \frac{d}{2t} \quad (3)$$

Table III. Crack growth parameters (Refs. 17, 18)

| Parameter | Minimum | Nominal | Maximum |
|---|---|---|---|
| $\alpha$ | 2.5x10$^{-2}$ | 2.8 x10$^{-2}$ | 3.1 x10$^{-2}$ |
| $k_{th}$ (MPa) | 8 | 9 | 10 |
| $\beta$ | 1.07 | 1.16 | 1.25 |
| $F$ | - | 0.93 | - |

Table IV. Tubes parameters

| Parameter | Nominal Value | Uncertainty [uniform distribution] |
|---|---|---|
| Outside diameter $d$ | 22.23 mm | +/- 0.5 mm |
| Thickness $t$ | 1.27 mm | +/- 12.5% |
| Nominal pressure difference $\Delta P_{nom}$ | 8.3 MPa | +/- 1 MPa |

The NRC requires inspecting the SG tubes using eddy current testing to determine the crack length, then during refueling (i.e., each 2 years), and plugging them if the crack length $a$ exceeds the value of 1.52 mm (Ref. 19). Otherwise, plugging is not enforced and cracks may continue growing during the following cycle, reducing the capability of the tube to withstand an overpressure induced by a SLB. Indeed, a rupture (and the following SGTR) occurs when the crack length $a$ exceeds the critical value $a_{cr}$ (plotted in Figure 3, for the case under analysis), that depends on the pressure difference $\Delta P$ in the tube wall during the accident scenario (Refs. 17, 20).

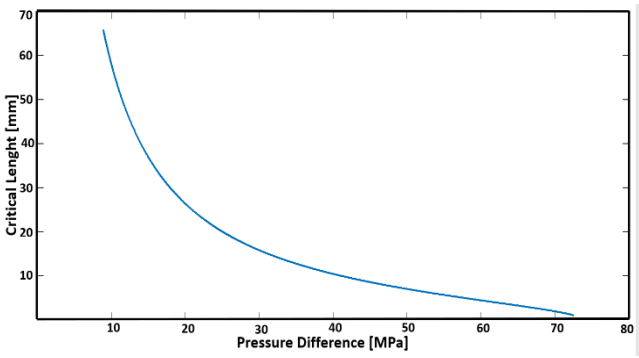


Figure 3. Critical crack length $a_{cr}$ in the SGTR, as a function of the pressure difference $\Delta P$ (Refs. 17, 20).

During the normal operation of the NPP, the degradation mechanism that affects the SG tubes is influenced by the operational pressure difference ΔP and $a$ has to be compared to the calculated $a_{cr}$ to ascertain whether the tube fails or not.

When a SLB occurs, the overpressure $\Delta P_{SLB} = \Delta P + \Delta P_{out,nom}$ (i.e., the pressure difference between the inner and the outer side of the SG tubes resulting from a complete depressurization of the secondary side of the SG) drastically reduces $a_{cr}$: Figure 4 shows in dashed-dotted line the evolution of $a_{cr}$ when the pressure difference changes from $\Delta P$ to $\Delta P_{SLB}$.

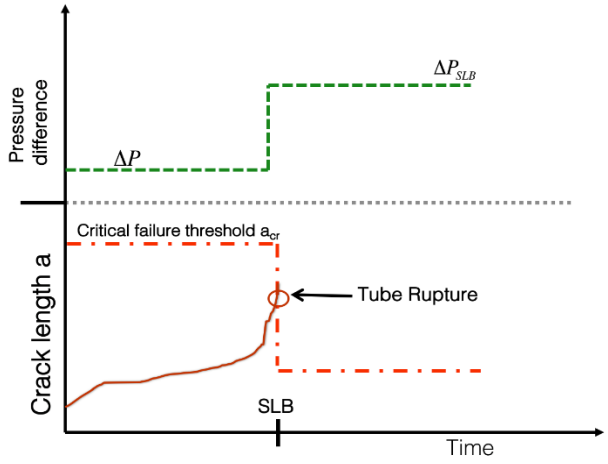


Figure 4. Crack growth (continuous line), pressure difference $\Delta P$ (dashed line) and critical value $a_{cr}$ during a SLB-induced SGTR accident scenario.

## III. ESTIMATION OF SGTR FREQUENCY

The estimation of the CDF due to the SLB-induced SGTR accident scenario is here performed by updating, at each refueling cycle, the likelihood of a SLB-induced SGTR based on the effective operative conditions that the NPP and its components are expected to deal with during

the following cycle. This approach enhances the latest NRC PSA approaches, which reflect the current design and configuration of the system enforcing NRC requirements (Ref. 2), by integrating degradation mechanisms, aging effects and accounting for the effects of the real system conditions.

The CB-PSA procedure that is here implemented is summarized as follows (Ref. 6):

1) At each inspection/refueling cycle *t*, simulate, for each tube, the onset, formation and propagation of the crack for the SG tube bundle up to the following inspection/refueling cycle *t*+1. For simplicity, each tube is considered to be independent from the others (thus, its state is not influenced by its neighbor tubes degradation states), but due account is given to the tubes stochastic degradation that proceeds, with parameters uncertainties as listed in Tables III and IV. In particular, since the tube bundle is affected by an evolving operative condition profile (i.e., the NPP power demand *W*) along the 40 years (20 cycles) SG lifetime, and power affects the pressure difference ΔP (that strongly influences the tubes degradation mechanism), we consider Eq. (4), that has been proposed and discussed in (Ref. 6), to hold for calculating the effective tube inner pressure $P_{in}$ under an effective *W* that differs from $W_{nom}$

$$\boldsymbol{P_{in} = P_{in,nom} \cdot \left(1 + \frac{W}{W_{nom}}\right)} \quad (4)$$

Figure 5 shows, without loss of generality, an example of the variation of *W* in the SG lifetime (hereafter assumed as reference load profile), whereas Figure 6 shows the resulting $\boldsymbol{\Delta P = P_{in} - P_{out,nom}}$ (continuous line), in comparison with the expected pressure difference under nominal conditions $\boldsymbol{\Delta P_{nom} = P_{in,nom} - P_{out,nom}}$ (dotted line).

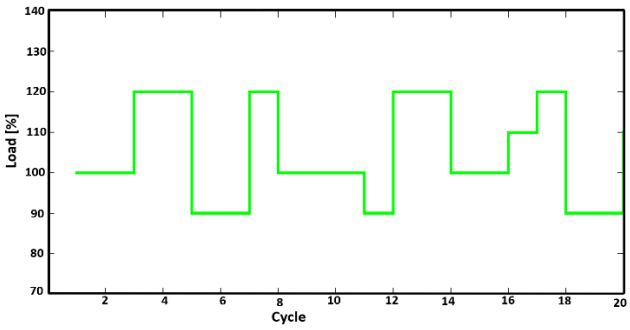


Figure 5. Reference load profile *W* along the 40 years NPP lifetime.

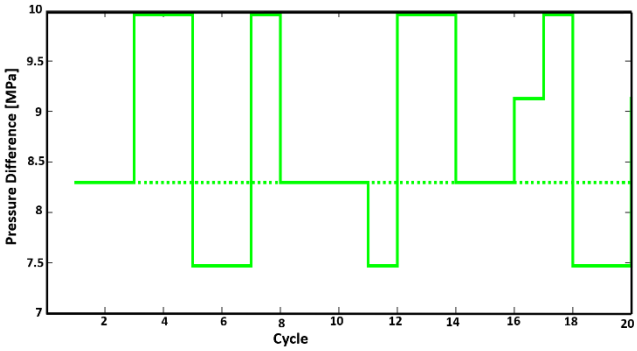


Figure 6. Pressure difference $\Delta P_{nom}$ under nominal conditions (dotted line) and pressure difference ΔP induced by the load variation (continuous line) during the 20 two-years cycles.

If we assume that cracks that at inspection time *t* exceed 1.52 mm are plugged according to the NRC requirement (Ref. 19), the number of tubes that are to be plugged is plotted in Figures 7.

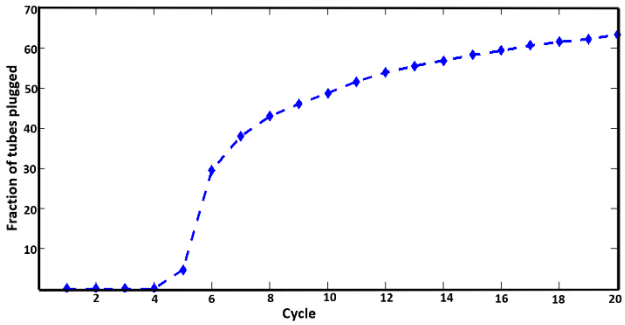


Figure 7. Fraction of the total number of tubes plugged at a given cycle over the total number of tubes.

If any tube has been plugged during inspections, the remaining tubes have to withstand an overpressure, as modelled in Eq. (5)

$$\Delta P = \mathrm{P}_{\boldsymbol{in}} \cdot \left(1 + \frac{N_{tb,plugged}}{N_{tb}} \cdot \gamma\right) - \mathrm{P}_{out,nom} \quad (5)$$

where the larger the number $N_{tb,plugged}$ of plugged tubes, the larger the ΔP.

The combination between the pressure difference resulting from the variations of *W* and the overpressure due to the plugging procedure allows calculating the resulting pressure difference. Figure 8, continuous line, shows the overall condition-dependent pressure difference that a tube (which is never plugged) has to withstand throughout a SG lifetime, when $\gamma$ in Eq. (5) is assumed to be equal to 0.4, the fraction of the total number of plugged tubes at each cycle (over the total number of available SG tubes $N_{tb}(t)$) is given in Figure 6 and is affected by the reference load profile of Figure 5.

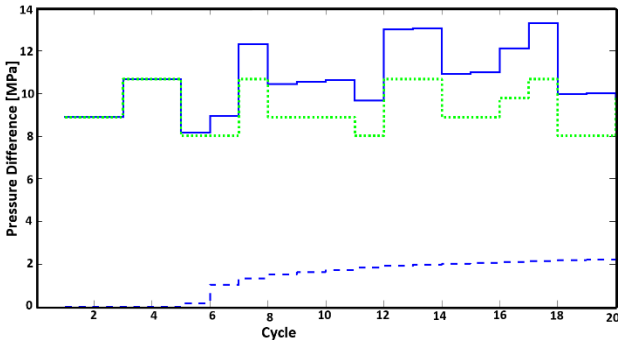


Figure 8. Pressure difference induced by the power variation (dotted line), pressure difference induced by the NRC plugging procedure (dashed line) and overall pressure difference that the tube has to withstand throughout the 20 cycles of the SG lifetime (continuous line).

When the SLB accident occurs, the pressure difference resulting from the depressurization of the secondary side of the SG becomes $\Delta P_{SLB} = \Delta P - P_{out,nom}$ (shown in Figure 9).

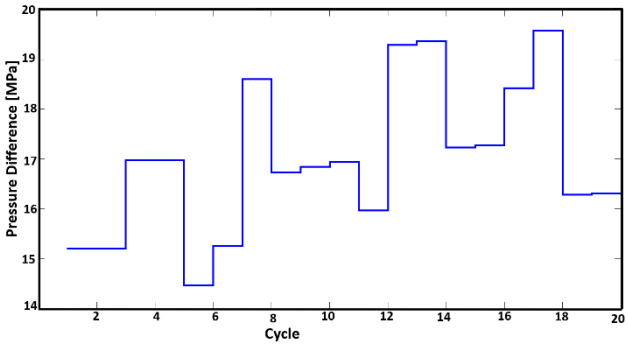


Figure 9. Pressure difference that the tubes have to withstand during a SLB accidental scenario, throughout the 20 cycles of the SG lifetime (continuous line).

At the *t-th* inspection time, the NRC requirement is enforced and the tube plugged if any of the simulated stochastic crack evolutions (continuous line in Figure 10) is found to exceed the plugging threshold (dotted line in Figure 10); otherwise, cracks continue to grow up to the following inspection time, leaving the SG exposed to the risk of cracks exceeding the critical length $a_{cr}$ (dashed line), that dynamically changes, depending on the condition-dependent pressure difference of Figure 9. We can notice that some cracks exceed the critical length $a_{cr}$, making the tubes likely to suffer a SLB-induced SGTR, as it occurs during the 6$^{th}$, 7$^{th}$, 8$^{th}$, 9$^{th}$, 10$^{th}$, 11$^{th}$, 12$^{th}$, 13$^{th}$, 14$^{th}$, 15$^{th}$, 16$^{th}$, 17$^{th}$, 18$^{th}$ cycles in Figure 10, for example.

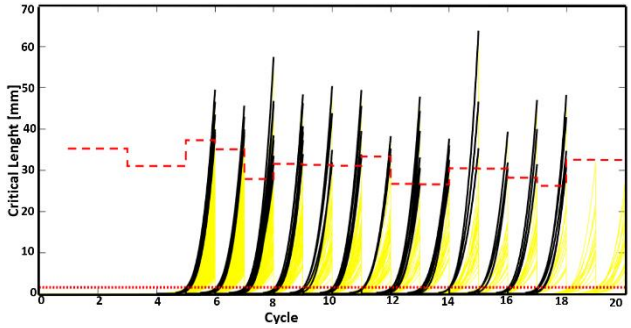


Figure 10. Simulated cracks evolution during the SG lifetime (continuous lines); plugging threshold (dotted line) and critical length $a_{cr}$ (dashed line), that dynamically changes due to the dependence on *W* and $\Delta P$.

2) Calculate the expected tube rupture frequency among the *t-th* and the *(t+1)-th* inspections by Eq. (6)

$$p_{tr}(t) = \frac{n(t)+1/2}{T \cdot N_{tb}(t)} \qquad (6)$$

where $N_{tb}(t)$ is the number of tubes that have not been already plugged at the *t-th* inspection and which have to withstand the overpressure calculated at step I, *N(t)* is the number of tubes that will reach $a_{cr}$ (according to the propagation model of Eq. (1)) and could originate a SGTR, in case of SLB accident, during the *t*-th cycle, *t*=1,2,…,*T*. Then, assuming the $N_{tb}(t)$ tubes to be independent, the SGTR frequency among the *t-th* and the *(t+1)-th* inspection is equal to $p_{SGTR}(t) = 1 - \prod_{N_{tb}}(1 - p_{tr}(t))$.

Figure 11 shows the $p_{SGTR}(t)$ obtained applying the CB-PSA framework (continuous line) for a SBL-induced SGTR, in comparison with the results obtained enforcing NRC requirements (e.g., evaluating the effects of the plugging procedure without considering the effective operative conditions of the NPP) (dashed line), the results for a spontaneous SGTR frequency (e.g., the SGTR frequency without considering the effects of a SLB) (dashed-dotted line) as evaluated in (Ref. 6) and the SGTR probability provided by a conventional PSA (dotted line). The $p_{SGTR}(t)$ value in the CB-PSA framework, for a SLB induced SGTR, is larger than the conventional PSA value because it considers the cracks onset, formation and propagation influenced by the overpressure induced by the plugging procedure, the power variations and the effects of the SLB. The comparison of the CB-PSA and the PSA enforcing the NRC requirements shows that CB-PSA realistically accounts for the occurred evidence and it is neither over-conservative nor under-conservative. One can also notice that the larger the value of ΔP (see also Figure 9), like during the 7$^{th}$, 12$^{th}$, 15$^{th}$, 16$^{th}$, 17$^{th}$ cycles, the larger the value of the CB-PSA $p_{SGTR}(t)$, with respect to $p_{SGTR}(t)$ obtained enforcing NRC rule.

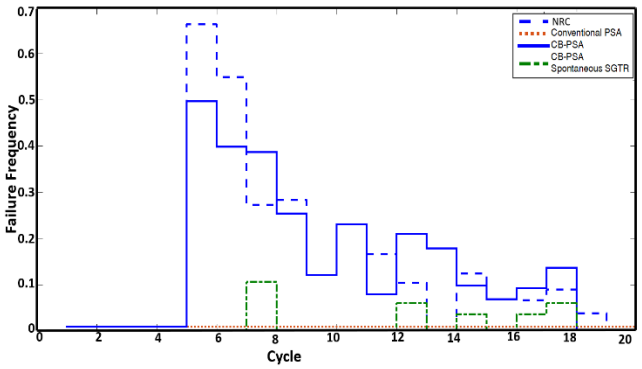


Figure 11. Condition-dependent likelihood of a SLB-induced SGTR (continuous line), SGTR probability resulting from conventional PSA (dotted line), $\boldsymbol{p_{SGTR}(t)}$ computed by enforcing NRC (dashed line) and spontaneous SGTR frequency (dashed-dotted line) (see (Ref. 6)).

Figure 12 shows that the CDF varies along *t* because of the dynamically changing estimation of $p_{SGTR}(t)$ . The comparison with the results provided by the conventional PSA and the enforcement of NRC rule shows their inability of accounting for the effects of the real system conditions.

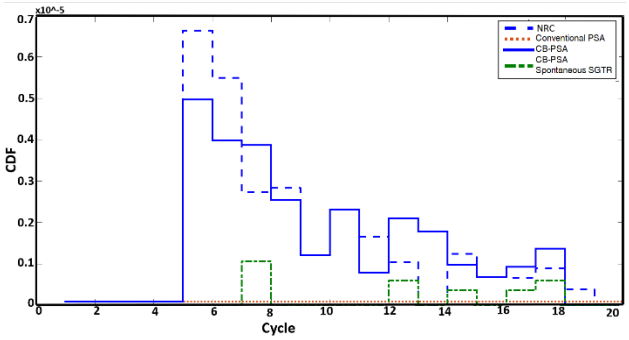


Figure 12. Comparison of the updated CDF resulting from the CB-PSA analysis (continuous line), the CDF resulting from enforcing NRC requirements, the CDF obtained by enforcing NRC requirements and the CDF of a spontaneous SGTR (dashed-dotted line) (see (Ref. 6)).

### III.A CB-PSA solution to optimize the plugging strategy and predict the escalation of a SLB-induced SGTR

The data collected during the inspections combined with the expected $\boldsymbol{p_{SGTR}(t)}$ results from CB-PSA can be used, firstly, for informing at each *t-th* inspection time the decision on whether to plug (or not) cracked tubes, and, then, to predict the time dependent evolution of the risk indicators (i.e., the likelihood of tube rupture) during the following cycle. In other words, we propose an optimization of the plugging strategy to control the escalation of potential SLB-induced SGTR.
The procedure of analysis goes as follows:

i. At each cycle *t*, simulate for each one of the $N_{tb}$ tubes of the SG bundle, the crack onset, formation and propagation as described in 1), accounting for the same dependences on *W* and $\Delta P$.

ii. At the end of each cycle *t*, during the inspection, collect the measurements of the crack lengths, that, even if found with *a* exceeding 1.52 mm, are not plugged. Then, for each crack, simulate $N_S$ alternative stochastic evolutions of the crack during the next *t*+1 cycle, to evaluate the probability that the crack length exceeds the critical length $a_{cr}$ during such cycle. Without loss of generality, Figure 13 shows an example of $N_S$ simulations (continuous lines) originated by the same crack initiated during a generic *t-th* cycle (dashed dotted line); the probability distribution of the crack length reached at the end of the *t*+1 cycle can be calculated, as well as the probability of exceeding the critical length $a_{cr}$ that causes the SGTR (dashed line) and the related likelihood (pdf highlighted area).

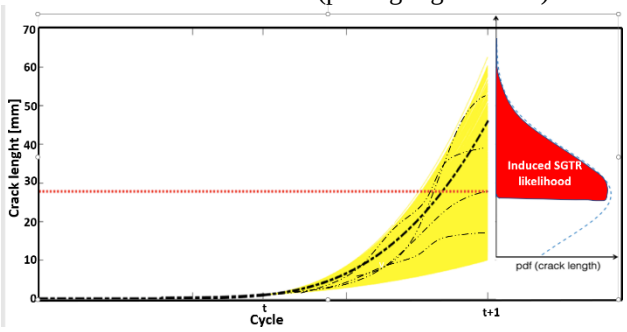


Figure 13. Simulated crack during a generic *t+1* cycle (continuous lines) and associated probability distribution for the crack length at the end of the cycle (continuous line on the right), compared with the critical length $a_{cr}$ that causes the SLB-induced SGTR (dashed horizontal line).

The simulations of Figure 13 provide also a time-dependent evaluation of the likelihood of a SLB-induced SGTR, along each cycle. Figure 14 shows an example: at the beginning of the cycle the simulated cracks are characterized by a low crack length, and, consequently, the likelihood of tube rupture is equal to 0. Then, the degradation mechanism, influenced by the pressure difference $\Delta P$, makes the crack grow and leaves the SG exposed to the risk of cracks exceeding the critical length $a_{cr}$ and, consequently, increases the likelihood of SLB-induced SGTR. In this way, CB-PSA is used to predict the evolution of the SGTR likelihood along the cycle, computing a time-dependent risk estimation.

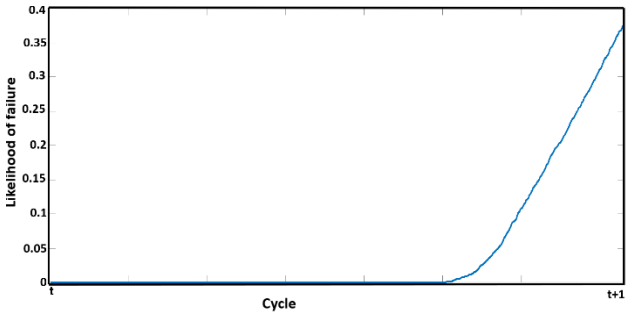


Figure 14. Time-dependent likelihood of SLB-induced SGTR, based on the simulations of Figure 17.

iii. Compute, for each tube, the 90-*th*-percentile of the probability distribution of the crack length that is reached at the end of the *t+1* cycle and plug the tube if this value exceeds the critical length $a_{cr}$ that could originate the SLB-induced SGTR under the expected pressure difference $\Delta P_{SLB}$ resulting from the depressurization of the secondary side of the SG.

iv. Calculate, based on iii, the likelihood of tube rupture $p_{tr}(t)$ between the *t-th* and *(t+1)-th* inspections (as in Eq. (8))

$$p_{tr}(t) = \frac{N(t)+1/2}{T \cdot N_{tb}(t)} \qquad (8)$$

The likelihood of a SLB-induced SGTR $p_{SGTR}(t)$ is, therefore, calculated as in Eq. (9)

$$p_{SGTR}(t) = 1 - \prod_{N_{tb}}(1 - p_{tr}(t)) \qquad (9)$$

v. At cycle *t*+1, proceed with step *i* above until *T* is reached, by setting the initial crack length equal to that found at the *t-th* inspection.

Figure 15 shows the $p_{SGTR}(t)$ obtained with the plugging optimization procedure (dashed-dotted line), the likelihood of a SLB-induced SGTR computed with the CB-PSA of Section 3 (continuous line) and the SGTR frequency resulting from a traditional PSA (dotted line). It is worth highlighting the reduction of the likelihood of a SLB-induced SGTR thanks to the proposed optimization of the plugging procedure.

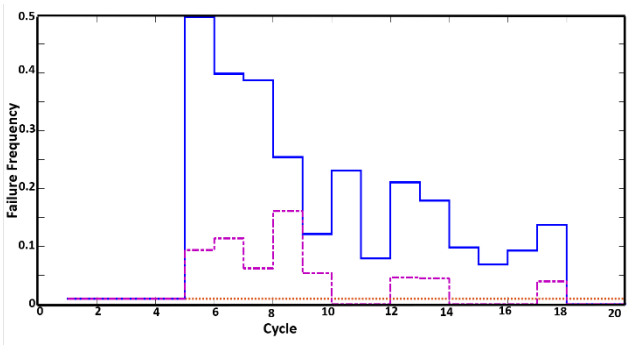


Figure 15. Comparison between the $\boldsymbol{p_{SGTR}(t)}$ obtained with the plugging optimization procedure (dashed-dotted line), the likelihood of a SLB-induced SGTR computed with the CB-PSA of Section 3 (continuous line) and the SGTR frequency resulting from a traditional PSA (dotted line).

As for CB-PSA, the dynamic updating of the predicted SGTR frequency (Figure 15) allows for a dynamic calculation of the CDF (Figure 16).

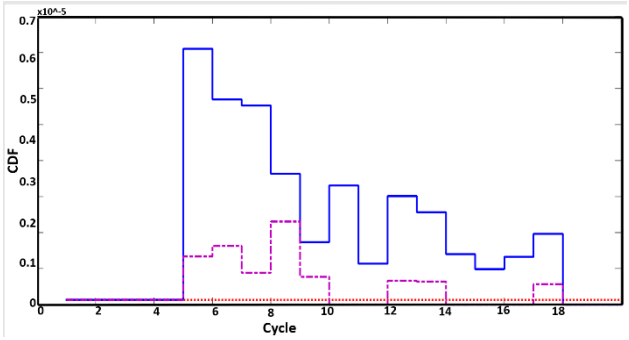


Figure 16. Comparison between the CDF obtained with the plugging optimization procedure (dashed-dotted line), the CDF computed with the CB-PSA of Section 3 (continuous line) and the CDF resulting from a traditional PSA (dotted line).

## IV. Conclusions

In this work, the SLB-induced SGTR accident scenario is considered within a CB-PSA framework. A model for the onset, formation and propagation of spontaneous cracks in the SG is used to dynamically update the likelihood of the SLB-induced SGTR throughout the system lifetime based on the cracks observations collected by inspection at the successive fuel cycle and the CDF is, then, updated based on the current state of the plant.
CB-PSA extends and advances latest PSA approaches currently used in NPPs. The degradation that affects the SG tubes and can cause the SGTR is duly accounted for by exploiting the condition-monitoring data.

**REFERENCES**

1. “Advances in reliability analysis and probabilistic safety assessment for nuclear power reactors” IAEA, IAEA-TECDOC-737, Vienna, 1994.

2. “Living probabilistic safety assessment (LPSA*)”,* IAEA, IAEA-TECDOC-1106, Austria 1999.

3. “A Living PSA system LIPSAS for an LMFBR”, *International symposium on the use of probabilistic safety assessment for operational safety*, Vienna (Austria); 3-7 Jun 1991.

4. IAEA. 2008 “PSA, Living PSA and Risk Monitoring, Key Differences and Conversion*”*, International Atomic Energy Agency, Vienna (Austria), Div. of Technical Co-operation Programmes; 248 p; 1997; p. 161-172; Workshop on PSA applications; Sofia (Bulgaria); 7-11 Oct 2008.

5. M. Zubair, Z. Zhang & S.U. Khan. 2011.“A methodology for Living Probabilistic Safety Assessment (LPSA) based on Advanced Control Room Operator Support System (ACROSS)”, *Annals of Nuclear Energy* vol. 38, Issue 6, June 2011, Pages 1351–1355.

6. F. Di Maio, F. Antonello & E. Zio. 2018. “Condition-Based Probabilistic Safety Assessment: a Spontaneous Steam Generator Tube Rupture Accident Scenario”. *Nuclear Engineering and Design vol. 326, 2018, p 41-54.*

7. P.V. Varde & M.G. Pecht. 2015. “Role of prognostics in support of integrated risk-based engineering in nuclear power plant safety*”, Nuclear Engineering and Technology*, vol. 47, Issue 2, March 2015, Pages 204–211.

8. T. Aldemir. 2013. “A survey of dynamic methodologies for probabilistic safety assessment of nuclear power plant”, *Annals of Nuclear Energy*, vol. 52, February 2013, Pages 113–124

9. S. Poghosyan & A. Amirjanyan. 2015 “Risk-informed Prioirtization of Modernization Activities Using Ageing PSA”, *Nuclear Engineering and Technology***,** vol 47, Issue 2, March 2015, Pages 204–21.

10. H. Kim, S.H. Lee, J.K. Park, Y.S. Chang & G. Heo. 2015. “Reliability Data Update Using Condition Monitoring And Prognostics In Probabilistic Safety Assessment*”, Nuclear Engineering and Technology* vol. 47, Issue 2, Pages 204–221.

11. E. Zio. 2016. “Some Challenges and Opportunities in Reliability Engineering”, *IEEE Transactions on Reliability*, vol. 65, Issue: 4, Dec. 2016

12. “Steam Generator Tube Failures”, U.S National Regulatory Commission, NUREG/CR-6365, Washington D.C., 1996.

14. R. Lewandowski. 2013. *“*Incorporation of Corrosion Mechanisms into a State-dependent Probabilistic Risk Assessment*”, The Ohio State University,* Ohio.

15. M.B. Sattison & K.W. Hall. 1989 ”Analysis of core damage frequency from internal events: Zion Unit 1*”,* U.S. Nuclear Regulatory Commission. Idaho.

16. “Rates of Initiating Events at U.S. Nulcear Power Plants: 1987e1995”, U.S National Regulatory Commission , NUREG/CR-5750, Washington D.C., 1998.

17. L. Cizelj & B. Mavko. 1995. “Propagation of stress corrosion cracks in steam generator tubes”, *International Journal of Pressure Vessels and Piping* 63(1), 1995, Pages 35-43.

18. R. Lewandowski, R. Denning, T. Aldemir & J. Zhang. 2016. “Implementation of condition-dependent probabilistic risk assessment using surveillance data on passive components”, *Annals of Nuclear Energy* 87, 690 - 760.

19. NRC by K.C Wade. 1995. “Steam generator degradation and its impact on continued operation of pressurized water reactors in the United States*”. Energy Information Administration/Electric Power Monthly*, August, 1995.

20. J.W. Hines, D. Garvey, J. Garvey & R. Seibert. 2008. “Technical Review of On-line Monitoring Techniques for Performance Assessment”, NUREG/CR-6895, vol. 3-Limiting Case Studies, U.S. Nuclear Regulatory Commission, Washington D.C., 2008.